Available online at www.sciencedirect.com
SCIENCE DIRECT
Polymer 46 (2005) 9053–9063
polymer
www.elsevier.com/locate/polymer

Electrochemical polymerisation of 5-amino-1,10-phenanthroline onto different substrates. Experimental and theoretical study

J.A. Cobos-Murcia[a], L. Galicia[a], A. Rojas-Hernández[a], M.T. Ramírez-Silva[a,*], R. Álvarez-Bustamante[b], M. Romero-Romo[b], G. Rosquete-Pina[b], M. Palomar-Pardavé[b,*]

[a]*Departamento de Química, Universidad Autónoma Metropolitana-Iztapalapa, San Rafael Atlixco No. 186 Col. Vicentina, C.P. 09340 México DF, México*
[b]*Departamento de Materiales, Universidad Autónoma Metropolitana-Azcapotzalco, Av. San Pablo No. 180 Col. Reynosa Tamaulipas, C.P. 02200 México DF, México*

Received 26 February 2005; received in revised form 23 June 2005; accepted 7 July 2005
Available online 10 August 2005

Abstract

The present work shows that the 5-amino-1,10-phenanthroline (5Aphen) molecule can be electrochemically polymerised, forming a conducting polymer, through potentiodynamic as well as potentiostatic methods onto different electrode substrates: (1) A composite formed by carbon paste in an epoxy matrix, (2) glassy carbon and (3) polycrystalline gold. From the analysis of the experimental potentiostatic current-time plots obtained using electrodes (2) and (3) it is shown that for both cases the formation mechanism of the polymer, (poly5Aphen) involves the simultaneous presence of an adsorption process, which seems predominant at times short enough to the start of the potential jump, and a three-dimensional, 3D, nucleation and growth process limited by the monomer diffusion toward the electrode's interphase. The mechanism suggests that the growth of the polymer takes place via direct incorporation of the monomer species. Studies carried out varying the angular speed of the vitreous carbon rotating disc electrode (RDE) showed that the limiting current increased directly proportional to the square root of the rotation frequency, as predicted by the Levich equation, thus indicating that the possible formation of intermediate oligomer species have a small effect on the polymer growth. A theoretical study of the monomer and some oligomers, through evaluation of the Fukui functions, allowed us to gain insight on the mechanism of polymerization of 5Aphen. It was found a linear oligomer species that adequately describe the experimental features found like the conducting nature of the polymer formed.

Keywords: Conducting polymers; Electrochemistry; Electrodeposition

1. Introduction

The formation of conducting polymer membranes has acquired recently significant importance for the fabrication of ion-selective sensors, ISS. Among others, those that use electrodeposited polypyrrol films onto a composite electrode based on carbon-epoxy resin have shown to be quite useful for the quantitative determination of amphiphilic molecules, or surfactants, in particular for the dodecyl sulphate ion [1]. Recently, Galicia-Luis et al. [2,3], showed that the 5-amino-1,10-phenanthroline (5Aphen) molecule is susceptible to electropolymerisation in aqueous medium over a carbon-paste electrode and that the resulting film has been proved to be useful as a proton sensor. Given the importance of such finding, it is of interest to study the mechanism and the formation kinetics of the said polymer film (poly5Aphen) and to show that there exists the possibility of formation onto other substrates. On consideration of the aforementioned, the present work, therefore, studies the electropolymerisation of the 5Aphen onto different substrates, and studies as well the mechanism for the electroformation based on the analyses of the potentiostatic current transients which were experimentally obtained, through the existing methods that successfully describe electrochemical formation of new phases [4–9]. The growth kinetics and mechanism of electrochemically formed new phases' nuclei, have been largely studied with respect to electrodeposition processes of metals, though the studies on the formation of new phases from the

* Corresponding authors.
E-mail addresses: mtrs218@xanum.uam.mx (M.T. Ramírez-Silva), mepp@correo.azc.uam.mx (M. Palomar-Pardavé).

0032-3861/$ - see front matter © 2005 Elsevier Ltd. All rights reserved.
doi:10.1016/j.polymer.2005.07.026

electrolisation of organic molecules are apparently, not as numerous [10–12]. Also, in this work, we have included a theoretical study concerning the density functionals theory (DFT) [13] which for the present case, allows a more fundamental understanding on the formation mechanism of the poly5Aphen.

2. Experimental

The electropolymerisation of the 5-amino-1,10-phenanthroline (5Aphen) was studied with cyclic voltammetry, CV and chronoamperometry, CA. The cell used was a typical three-electrode cell arrangement with a Radiometer saturated mercury sulphate as reference, SMS, a BAS electrochemistry platinum wire as counter electrode. Also, the cell had a nitrogen bubbler to deareate the working solutions. The potential applied to the working electrodes was controlled by means of AUTOLAB PGSTAT 100 potentiostat-galvanostat connected through a PC with the General Purpose Electrochemical System (GPES) Version 4.9 Chemie B.V to implement the control modes elected and data acquisition. The following were the working electrodes, WE.

2.1. Carbon paste electrode

To fabricate this electrode a 5 cm long polyethylene tubing having 4 mm ID served to accomodate, as in a mold, the copper connecting wire and the mix composed of 1:0.7 carbon powder (Johnson Mathey, microcrystalline grade, 99.9995%) and mineral oil (Fluka), following the procedure established by Galicia et al. [2].

2.2. Glassy carbon electrode

This was the tip of a commercial Tacussel rotating disc with a 0.0707 cm^2 geometric area.

2.3. Polycrystalline gold

Also, this was the tip of a commercial Tacussel rotating disc electrode with a 0.0707 cm^2.

2.4. Carbon-epoxy resin composite

The cylindrical geometry was achieved by using a 6 mm ID PVC tube and 2 cm long, with a copper connection located at the centre on the opposite base of the cylinder, where the working surface is exposed. The mix used was a 1:1 graphite powder with epoxy resin from Araldite with H: R. hardener, both mixed in the 1:0.4 ratio. Once the mix had been prepared it was poured in the PVC tube and left to cure within an over at 60 °C during 24 h; see Fig. 1. Afterwards, the electrode surface was ground and polished to attain a smooth surface.

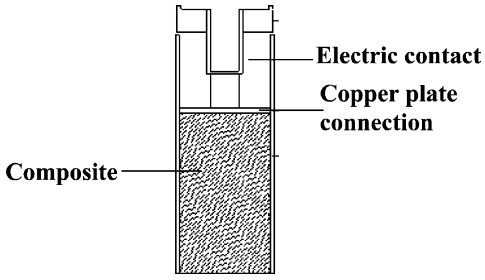

Fig. 1. Schematics of the experimental design of the composite electrode, which shows its various constituents.

Every electrode, except for the carbon paste one, was polished with 0.5 μm alumina before each experiment. In this same sense, the surface of the carbon paste electrodes was mechanically regenerated by sliding it under hand pressure over a filter paper, thus eliminating residues from the previous experiment.

The electropolymerisation of the 5Aphen on the implemented working electrodes was studied by using a 2×10^{-3} M 5Aphen (Polysciences Inc., analytical grade) aqueous solution and 0.5 M H_2SO_4 (Merck, analytical grade) at a pH = 0.3. All solutions were prepared with deionised water, 18.2 MΩ, free from organic matter, obtained from a US Filter PURELAB Plus UV equipment, deareated with nitrogen.

For those cases when the electrode's angular velocity was controlled, a BASi RDE-2 was used. It allows to impose fixed rotation rate to the working electrode in the ranges of 50–10,000 rpm at better than 1% accuracy.

3. Results and discussion

3.1. Thermodynamic study

Galicia-Luis et al. [2] and Gómez-Hernández [14] showed that the thermodynamic approach based on the construction of Predominance Zone Diagrams, PZD, constructed in accordance with the postulates of the Rojas-Hernández et al. [15] theory, allowed to establish that the 5Aphen's wholly protonated species was predominant at pH < 0.91 (Fig. 2). According with the authors, this is the species from which the growth of the film formed through electropolymerisation of the molecule that exhibits the best features and stability, which explains why such a pH range was used for the present study.

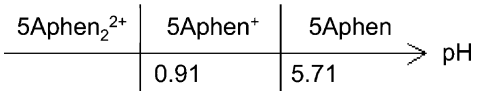

Fig. 2. Linear predominance zone diagram for the 5Aphen.

3.2. Potentiodynamic study

3.2.1. Influence of substrate's nature on the oxidation of the 5AphenH$_2^{2+}$

Fig. 3 shows the linear sweep voltammograms obtained during the oxidation of 5AphenH$_2^{2+}$ on different substrates, where all cases revealed the presence of the anodic peaks, p_a, which appear to present themselves approximately at 650 mV. However, it can be noted that the potential at which the oxidation process for the 5AphenH$_2^{2+}$ begins depends on the nature of the substrate. Further, it can be noted that the oxidation on the composite electrode appeared energetically favoured, as can be seen in Fig. 3(b), whereas from Fig. 3(d) it becomes apparent that the oxidation process taking place on the gold electrode appeared, energetically, more difficult.

3.2.2. Electropolymerisation of the 5AphenH$_2^{2+}$

Fig. 4 shows the cyclic voltammograms obtained with the system working electrode/aqueous solution of the 5Aphen for the different substrates considered. Each case indicates that 40 identical potential cycle sets were applied for three of them, except for the gold electrode. It is relevant to underline that the features observed in the plots 4(a), 4(b) and 4(c) are characteristic of the growth processes for conducting polymers, namely, the charge increments observed, cathodic inasmuch as anodic, with the number of potential cycles applied [16,17]. Fig. 4(d) for the gold electrode can be compared with voltammograms obtained with and without (blank) the 5Aphen. The peak p_a only appeared in the presence of the 5Aphen, however, the second anodic peak that formed when there was 5Aphen available in solution is due not only to oxidation of the molecule but also to oxidation of the substrate. It should be noted that, in comparison with the reduction peaks in Fig. 4(d), that the oxidation of gold appeared inhibited in the presence of the 5Aphen.

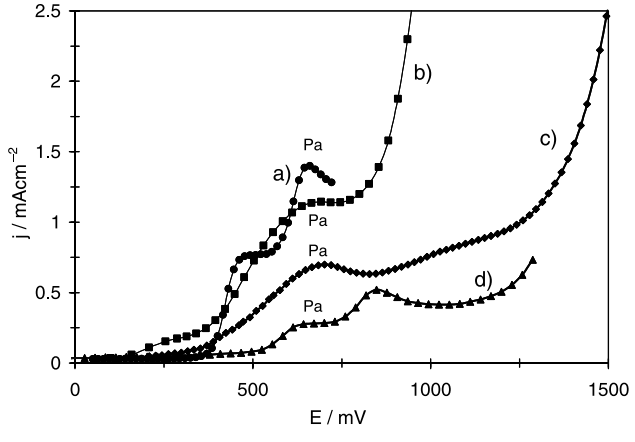

Fig. 3. Linear voltammograms obtained in the system working electrode/aqueous solution 5Aphen 2×10^{-3} M in 0.5 M H_2SO_4, pH = 0.3, where the electrodes were as follows: (a) Carbon paste, (b) graphite-epoxy resin composite, (c) glassy carbon and (d) polycrystalline gold. The potential scan started at the null current potential, OCP, respect to the anodic direction at a 100 mV s^{-1} rate.

3.3. Potentiostatic study

Fig. 5 shows the potentiostatic transients obtained during oxidation of the 5AphenH$_2^{2+}$ over the substrates herein considered. It can be observed that for times longer than 20 s, the *j–t* curves that result when the glassy carbon, see Fig. 5(c), and the gold electrodes were used, see Fig. 5(d), exhibit the characteristic features described for multiple nucleation processes of new phases, with 3D diffusion limited growth, as indicated by Scharifker et al. [4,5], Palomar-Pardavé et al. [8]. For both times longer and shorter than 20 s the transients displayed a current drop. Such type of transients have been reported previously by Mendoza-Huizar et al. [18] for Co electrodeposition onto gold, by Garduño-Juarez et al. [19] and by Garfias-Garcia et al. [20] for the electropolymerisation of a new conducting polymer based on Pb-acetate and by Ramírez et al. [21] during the electronucleation of silver onto glassy carbon. For all cases mentioned, it has been demonstrated that a model involving the simultaneous presence of an adsorption process and a 3D diffusion-limited nucleation, adequately represent the experimental evidence. Further, the *j–t* plots obtained from the carbon paste electrode see Fig. 5(a), and those from the composite electrode, see Fig. 5(b), do not present such characteristics. This may be due to 5AphenH$_2^{2+}$ polymerisation onto carbon paste and the composite electrode that occurs with a much faster kinetics than on the other substrates. It has been shown that when an electrochemical nucleation process increases its kinetics, for instance, occurring with a higher nucleation rate (A), then the maxima of the corresponding current transients appear, each time, with a higher current density and at lower times, see for instance: Fig. 2 in Ref. [8] and Fig. 3 in Ref. [18] or [21].

This work will only delve into the study of the *j–t* plots, which exhibit the typical nucleation characteristics, leaving the others for a later study.

In agreement with the model that describes the simultaneous presence of an adsorption process and one 3D nucleation process during the electrochemical formation of phases, for more details please refer to Mendoza-Huizar et al. [18] and Ramírez et al. [21], the overall current density is described by the following expression:

$$j_{total}(t) = j_{ad}(t) + j_{3D-dc}(t) \quad (1)$$

where $j_{ad}(t)$ is given by the equation: [22]

$$j_{ad} = k_1 \exp(-k_2 t) \quad (2)$$

where k_1 is the initial current density and k_2 is the time constant associated to the adsorptive pseudocapacitance. The $j_{3D\text{-}dc}(t)$ corresponds to that proposed by Scharifker et al. [4] to describe the potentiostatic current transients due to nucleation of 3D centres with growth limited by diffusion of

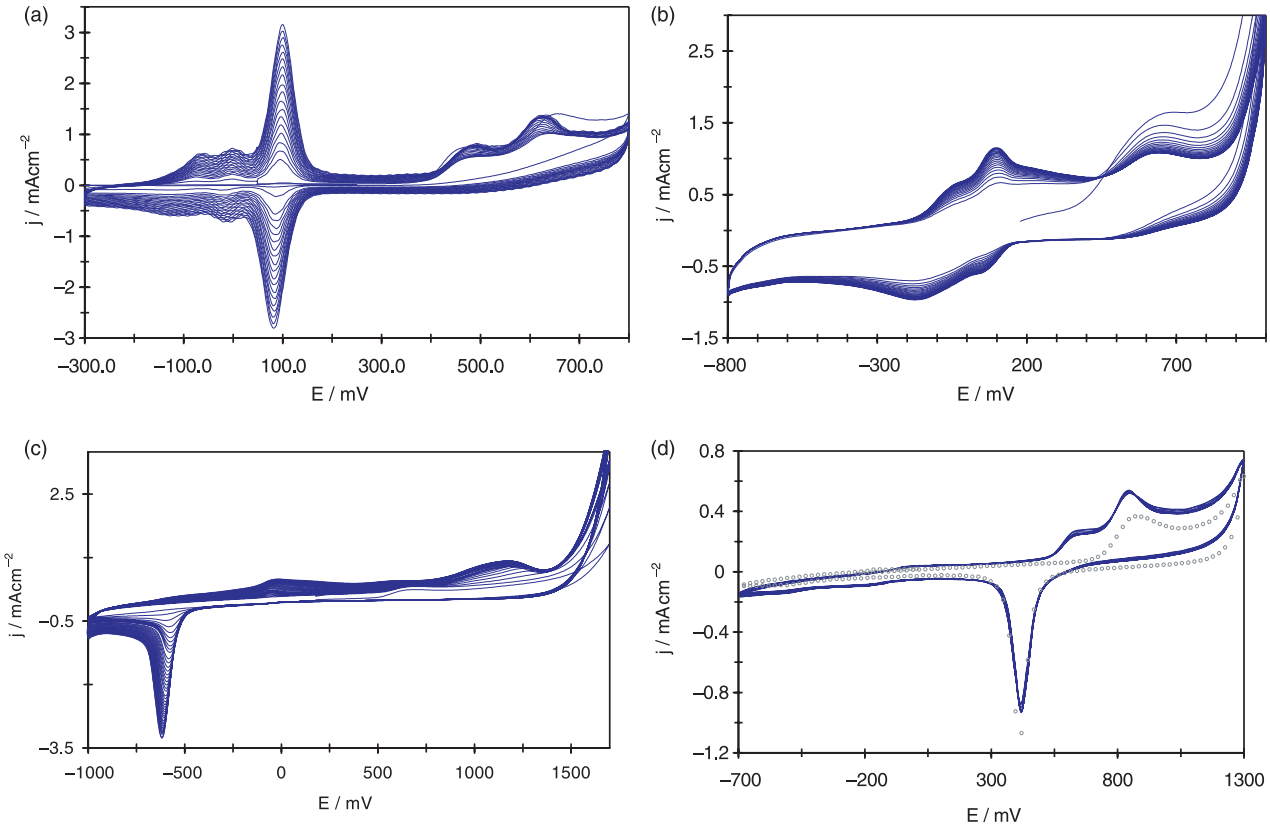

Fig. 4. Typical cyclic voltammograms obtained during the electropolymerisation with 2×10^{-3} M 5Aphen in sulphuric acid media, pH = 0.3 over different substrates: (a) Carbon paste, (b) graphite-epoxy resin composite, (c) glassy carbon and (d) polycrystalline gold, with (line) and without (points) 5Aphen in solution. The potential scan rate was 100 mV s^{-1}. (a)–(c) Show the result of scanning the potential during 40 cycles in the ranges thus indicated in each.

the electrodepositing species, which is given by the following equation:

$$I_{3D-dc}(t) = P_1 t^{-1/2}\left(1-\exp\left\{-P_2\left[t-\frac{1-\exp(-P_3 t)}{P_3}\right]\right\}\right) \quad (3)$$

with

$$P_1 = \frac{zFD^{1/2}c}{\pi^{1/2}} \quad (4)$$

$$P_2 = N_0\pi\left(\frac{8\pi M}{3\rho}\right)^{1/2} D \quad (5)$$

$$P_3 = A \quad (6)$$

In the present case zF in Eqs. (4)–(6) is the charge transferred per mol of transformed substance during the oxidation process of the 5Aphen, N_0 is the number density of active nucleation sites over the surface of the substrate, A is the nucleation rate, ρ and M are the density and atomic mass of the deposit monomer, respectively, D is the diffusion coefficient and c is the 5AphenH_2^{2+} concentration in the bulk solution.

3.3.1. Nucleation of the 5AphenH_2^{2+} onto gold

Fig. 6 shows the comparison between an experimental transient obtained during the oxidation of the 5AphenH_2^{2+} over the gold electrode and the one generated through non-linear fitting the experimental data to Eq. (1). It can be observed that the experimental evidence is adequately represented by the fitting procedure adopted.

3.3.2. Nucleation of the 5AphenH_2^{2+} onto glassy carbon

Fig. 7 shows the comparison between the theoretical transient generated through non-linear fitting to Eq. (1) of the experimental data generated during the electropolymerisation of the 5Aphen onto the glassy carbon electrode, after applying a 1500 mV potential. The parameters which rendered the best fit are shown in Table 1, which demonstrates that the model proposed is quite adequate to describe the process.

It is important to note that the value of the P_1 parameter, see Table 1, significantly changes with both substrate and potential. Since this parameter is directly related to the diffusion coefficient, D, of the depositing species, Eq. (4), then these results may indicate that different lengths (n) of soluble oligomer species (Mo_n) were formed during the initiation stage of the polymerisation process, see below,

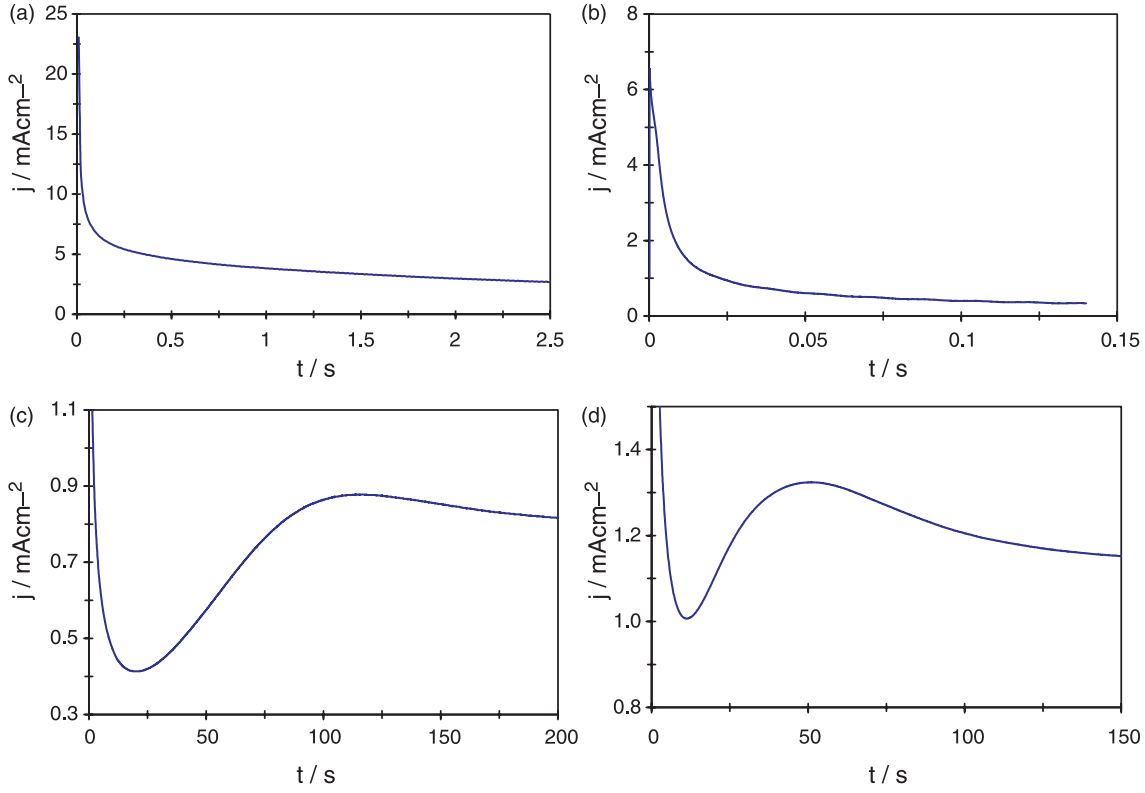

Fig. 5. Typical experimental chronoamperograms obtained during the electropolymerisation with 2×10^{-3} M 5Aphen in aqueous solution at pH=0.3, over different substrates: (a) Carbon paste, (b) graphite-epoxy resin composite, (c) glassy carbon and (d) polycrystalline gold. The potential jumps applied to obtain these transients were as follows: (a) 50 mV (ocp)→800 mV, (b) 179 mV (ocp)→500 mV, (c) 177 mV (ocp)→1500 mV, and (d) −207 mV (ocp)→1440 mV.

depending on the value of the applied potential and the substrate used for polymerisation, because according to the Stokes–Einstein equation, see Eq. (7), D is inversely proportional to the hydrodynamic radius, R_H, of the diffusing species.

$$D = \frac{kT}{6\pi\nu R_H} \tag{7}$$

where k is the Boltzmann constant, T is the absolute temperature, and ν is the viscosity of the solution.

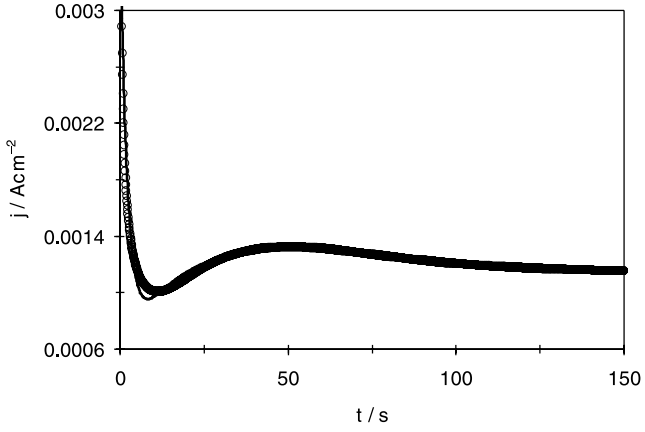

Fig. 6. Comparison between an experimental potentiostatic current density (○) obtained during the electropolymerisation of the 5Aphen in the system: Polycrystalline gold/2×10^{-3} M 5Aphen aqueous solution in 0.5 M sulphuric acid, pH=0.3 after imposing a potential jump from the null current potential (−207 mV) to a potential of 1450 mV and a theoretical transient (——) generated through non-linear fitting the experimental data to Eq. (1). The parameters, which rendered the best fit are summarised in Table 1.

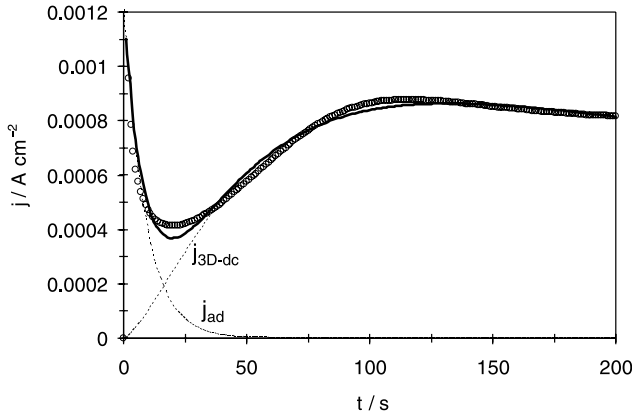

Fig. 7. Comparison between an experimental potentiostatic current transient (○) obtained during the electropolymerisation of the 5Aphen in the system: Glassy carbon/2×10^{-3} M 5Aphen in sulphuric acid at pH=0.3, after imposing a potential jump from the null current potential 177 mV to a 1500 mV, and the theoretical transient (——) that resulted from the non-linear fitting the experimental data to Eq. (1). The parameters, which gave the best fit are shown in Table 1. Individual contribution to the total current is also shown in the figure.

Table 1
Variation of the non-linear fitting parameters from the Eq. (1) applied to the experimental data of the transients obtained during the electropolymerisation of the 5Aphen as a function of the nature of the substrate and of the applied potential

Substrate	E (mV)	$10^3 k_1$ (A cm^{-2})	$10k_2$ (s)	$10^3 P_1$ (A cm^{-2} s$^{-1/2}$)	$10^2 P_2$ (s^{-1})	P_3 (s^{-1})
Gold	1450	3.0±0.01	4.8±0.06	5.6±0.01	3.5±0.01	0.14±0.006
Glassy carbon	1500	1.2±0.01	1.1±0.02	12.4±0.1	1.5±0.04	0.04±0.002
	1650	17±0.11	11.8±0.80	30.0±0.2	15.8±0.5	3.1±1.3

A pathway for the electrochemical formation of conducting polymers involves two stages that can be described as follows [23,24]

Initiation

$$2Mo_{(aq)} \rightleftarrows 2Mo^{\cdot+}_{(aq)} + 2e^- \quad (8)$$

$$2Mo^{\cdot+}_{(aq)} \rightleftarrows Mo^{2+}_{2(aq)} \quad (9)$$

$$Mo^{2+}_{2(aq)} \rightleftarrows Mo_{2(aq)} + 2H^+ \quad (10)$$

Propagation

$$Mo_{n(aq)} \rightleftarrows Mo^{\cdot+}_{n(aq)} + e^- \quad (11)$$

$$Mo_{j(aq)} \rightleftarrows Mo^{\cdot+}_{j(aq)} + e^- \quad (12)$$

$$Mo^{\cdot+}_{n(aq)} + Mo^{\cdot+}_{j(aq)} \rightleftarrows Mo^{2+}_{j+n(aq)} \quad (13)$$

$$Mo^{2+}_{j+n(aq)} \rightleftarrows Mo_{j+n(s)} + 2H^+ \quad (14)$$

$$Mo_{j+n(s)} + Mo_{(aq)} \rightleftarrows Mo_{((j+n)+1)(s)} + 2e^- + H^+ \quad (15)$$

$$Mo_{j+n(s)} + Mo_{n(aq)} \rightleftarrows Mo_{((j+n)+n)(s)} + 2e^- + H^+ \quad (16)$$

In reactions (8)–(16), $Mo_{(aq)}$ represents the monomer species in solution, $Mo^{\cdot+}_{(aq)}$ a cation radical formed by the oxidation of the monomer and $Mo_{2(aq)}$ are the dimer in solution, $Mo_{n(aq)}$ and $Mo_{j(aq)}$ represent different oligomers in solution and $Mo_{j+n(s)}$ is an insoluble oligomer. Note that reactions (15) and (16) involve the growth of the polymer film through direct incorporation of the monomers (15) and/or oligomers in solution (16), which necessarily implies that the insoluble oligomers formed are behaving as a conducting phase.

3.4. Rotating disk electrode

3.4.1. Potentiodynamic study

Fig. 8 shows the linear voltammetry, LV, in the system glassy carbon/5Aphen at different angular speeds (ω). It is important to realize that the current densities j increase as the rotation speeds do so. This fact is clearly in contrast with what was noted by Scharifker et al. [23,24], who studied the pyrrole electropolymerisation process in the system glassy carbon/3.6×10^{-2} M pyrrole and 1 M KNO_3 and found the opposite, namely that the anodic current decreased as the rotation speed of the glassy carbon electrode increased. The authors showed that likely this was because polypyrrole formation requires prior formation of oligomers that may be forced away from the electrode's surface due to agitation, which in turn will decrease the associated current. This did not occur in the present case, thus it is plausible to think in terms of poly5Aphen's formation taking place due to direct monomer incorporation. This would account for the current density increase associated to a rotation speed increase of the electrode.

3.4.2. Potentiostatic study

Fig. 9 shows the potentiostatic current density transients obtained during the oxidation of $5AfenH_2^{2+}$ over the glassy carbon electrode at different rotation speeds (ω). Like in the case of the linear sweep voltammograms, the stationary currents, $j_{L,}$ increase directly proportional to the square root of the rotation frequency, $f=\omega/2\pi$, see Fig. 10, as predicted by the Levich equation (17). However, it is clearly apparent that contrary to what can be expected from Eq. (17), the intercept of the current at zero rotation rate is different from zero, this can be ascribed to edges-related radial diffusion to the electrode, that the Levich equation (17) does not take into consideration when rotation rate of the electrode tends to zero. Another possibility can be the presence of a strong adsorption process. It is important to mention that the model herein proposed to describe the current due to the polimerisation process, see Eq. (1), already takes into consideration such a contribution

$$j_L = 0.620zFD^{2/3}\nu^{-1/6}c\omega^{1/2} \quad (17)$$

where j_L is the current density limit and ω is the angular speed of the electrode. Unless otherwise stated, the other terms have the usual meaning.

The results support the idea that the polymerisation of the 5Aphen is effected by means of the direct incorporation of the monomer. Thus they also give support to our previous simulation of the polymerisation mechanism of the 5Aphen, carried out with the aid of the nucleation and growth models.

3.5. Theoretical studies

To estimate the active sites pertaining to the 5Aphen

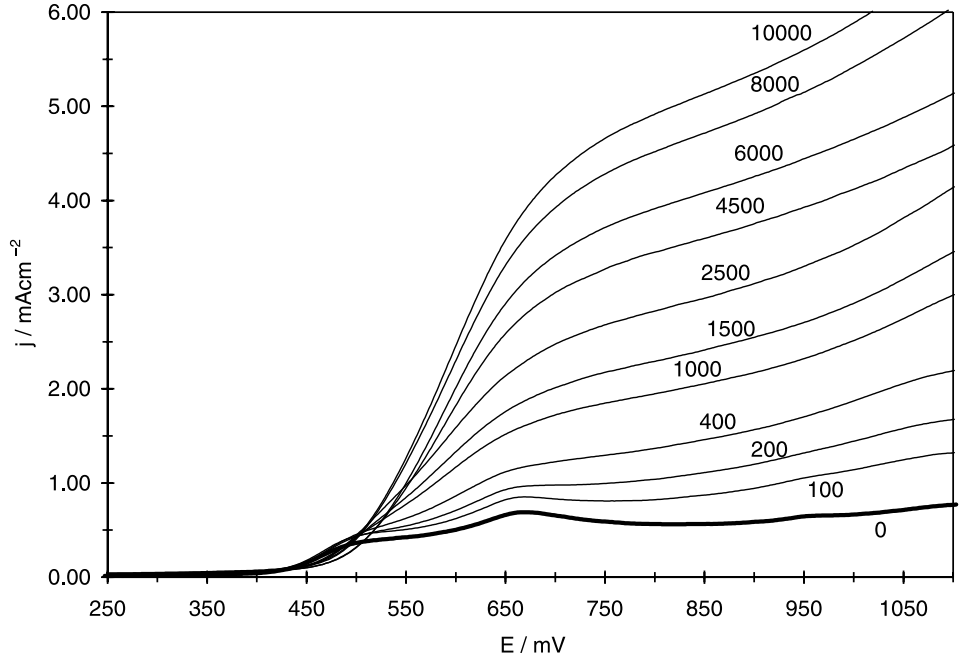

Fig. 8. Typical linear voltammograms obtained during the electropolymerisation of 5Aphen 2×10^{-3} M in sulphuric acid media, pH = 0.3 over a glassy carbon rotating disc electrode, GCRD, for different rotating speed, shown in the figure in rpm.

monomer [25–27], see Fig. 11(a), and with them the possible mechanism followed by the polymerisation reaction, a parameter was devised from the DFT [13]: The Fukui functions (*f*), using the frontier orbitals HOMO and LUMO, derived from the AM1 semiempirical method [28]. In order to do this, we have proceeded herewith to carry out an overall geometry optimisation through semi-empirical calculation AM1 for all the molecules, through the software ARGUSLAB 4.0 [29–32] running on a Pentium 4 PC having a 1.9 MHz and 500 Mb RAM.

The said Fukui functions give useful information on how the electron density (ρ) responds to the variations of the number of electrons (N), at constant external potential (v), as given by the following expression:

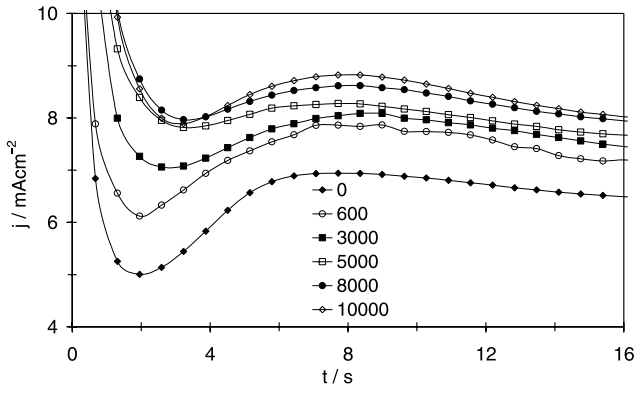

Fig. 9. Current density transients obtained during the electropolymerisation of 2×10^{-3} M 5Aphen in sulphuric acid media at pH = 0.3 after imposing a potential jump to reach 1650 mV on a rotating glassy carbon disc electrode, applying different rotation speeds, as indicated in the figure in rpm.

$$f(r) = \left[\frac{\partial\rho(r)}{\partial N}\right]_v \tag{18}$$

where r is the space co-ordinate.

It has been shown [33–36] that this parameter allows evaluation of the location of an active site, specific to a given molecule.

It is particularly important to underline that, formation of the polymer studied so far, necessarily begins with oxidation of the monomer, 5Aphen, which justifies taking into consideration the possibility of electron transfer to any site of the molecule, dependent on the charge changes and on the multiplicity. With this into consideration, the aforementioned Fukui function, was evaluated with Eq. (19):

$$f_{N_s}(r) = \left[\frac{\delta\rho(r)}{\delta N_s}\right]_N \tag{19}$$

where f_{N_s} is the Fukui function that takes into consideration the charge changes and the multiplicity, and N_s is the number of unpaired electrons.

3.5.1. Monomer of 5Aphen

The optimum geometry of 5Aphen molecule, AM1, is shown in Fig. 11(b).

The distribution of electrophilic and nucleophilic active sites is related to the values of the Fukui functions in one space region, namely, where this is positive (indicated in blue in Fig. 12) it would correspond to a locally nucleophilic site, while for a negative value (indicated in red, Fig. 12) this would correspond to an electrophilic site. The analysis of the Fukui function $f_{N_s}(r)$ for the 5Aphen, as shown in

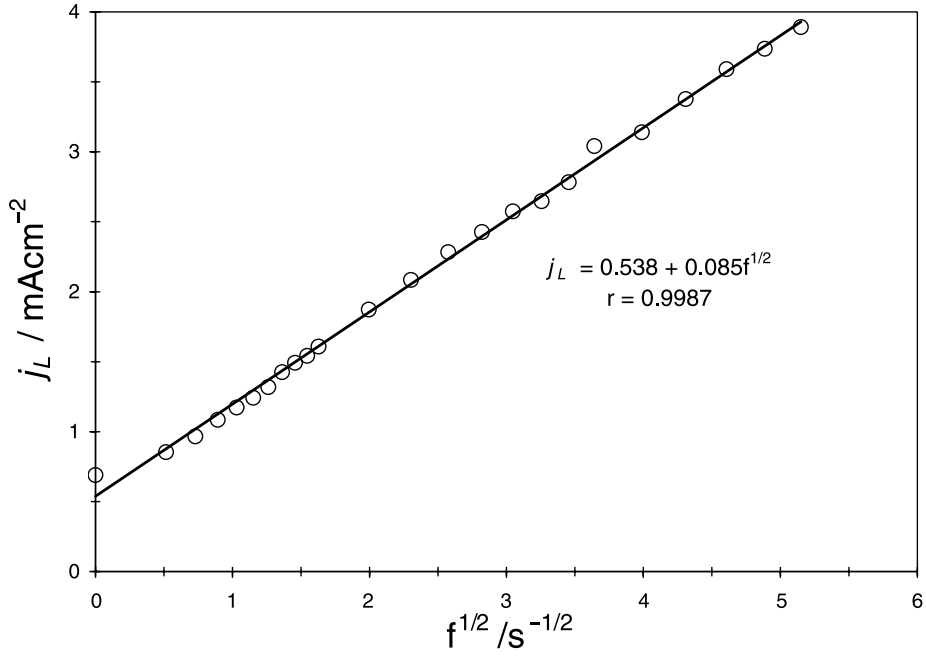

Fig. 10. Variation of the limiting current density or the stationary current of the experimental potentiostatic transients shown in Fig. 9 with the rotation frequency (open circles). The straight line represents the linear fit of the experimental data to the corresponding equation.

Fig. 12, indicates the presence of nucleophilic active sites on the following atoms: N_B, N_C, C_1, C_4, C_8 and C_{11}, meanwhile for the electrophilic reaction, the active sites would be: N_A, C_6 and C_{10}, see Fig. 12. Oligomer formation will occur through the interaction of a nucleophilic site in one molecule with the electrophilic site on another. Thus, there would be 18 possible interactions, however, due to sterical effects the most likely ones would be: N_C–C_{10} and C_1–C_{10}.

The dimers related to such interactions and their formation energies are shown in Fig. 13, where it can be observed that the most stable structure is that formed by the latter interaction. Thus, growth of the polymer would occur through sites C_1 and C_{10}. It is important to stress out that Mora et al. [26] also concluded, from an ab initio quantum mechanical calculations, with unrestricted Hartree–Fock (HF) and Møller–Plesset perturbation theories, study of the 5Aphen monomer, that the polymerisation has a high probability of occurring at the C_1 or C_{10} atom.

3.5.2. Oligomers of the 5Aphen

With the criterion just outlined, the corresponding polymers were generated, bonded by the interaction C_1–C_{10}, from 2 to 6 units, that were fully optimized through the semi-empirical method AM1 followed by a Fukui calculation. The analysis of the functions permitted to find that the distribution of active sites in the said oligomers was dependent on the number of constituting units. The oligomers with a pair of units, see Fig. 14, present its active sites on the edges of the molecule, whereas those conglomerates formed by an odd number of units present its active sites within the central unit, specifically at the N_C, which apparently would be the one sterically favoured.

However, polymerisation from the three-unit oligomer

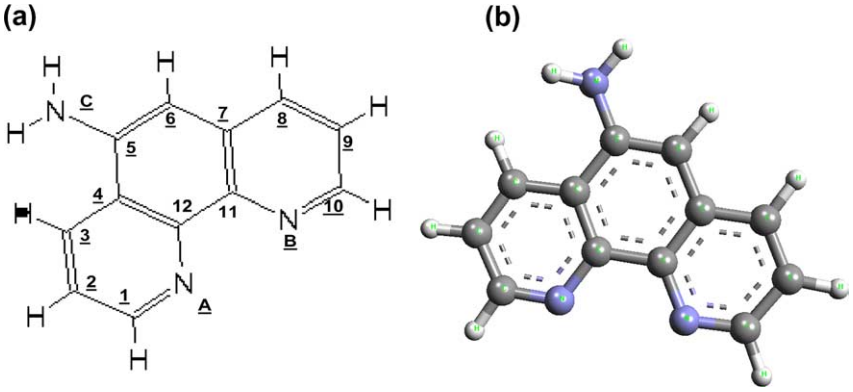

Fig. 11. (a) Molecular scheme of the 5Aphen (b) minimal energy conformation of 5-amino-1,10-phenanthroline obtained by AM1.

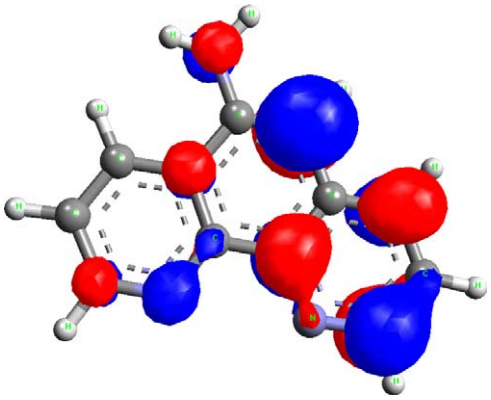

Fig. 12. Fukui function, $f_{N_s}(r)$, distribution of the 5Aphen monomer. In blue is indicated the space region where f_{N_s} is positive, nucleophilic site and in red where it is negative, electrophilic site.

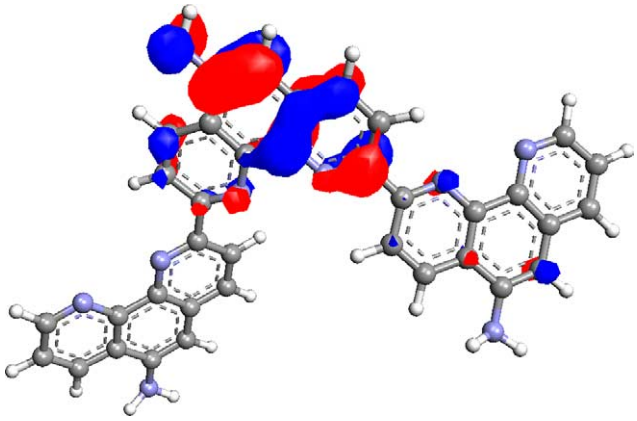

Fig. 14. Fukui function, $f_{N_s}(r)$, distribution of a 5Aphen trimer. The nucleophilic site corresponding to the space region where f_{N_s}, is positive, is indicated in blue and in red where it is negative, the electrophilic site.

with an electrophilic active site on the $N_{\underline{C}}$ would not really be possible, as it would require an interaction with the $C_{\underline{10}}$ which leads, as proven before, to energetically unfavourable structures.

In agreement with the Fukui functions, the even-numbered oligomers locate their active electrophilic sites on the $C_{\underline{1}}$, $C_{\underline{2}}$, $C_{\underline{9}}$ and $C_{\underline{10}}$, as indicated in Fig. 15 that shows a hexamer molecule. The previous result together with the fact that the resulting structure appeared 'W'-shaped, with an energy $\Delta H_f(\mathrm{AM1}) = -534.4082$ kcal mol^{-1} obtained through full optimisation of the hexamer that imposes a greater steric impediment on the polymer system making chains' crosslinking difficult, strongly suggests the existence of such a kind of electropolymerisation for the 5-amino-1,10-phenanthroline, 5Aphen.

When considering the definition of the Fukui function, see Eq. (18), it becomes possible to infer that in the regions where the Fukui is zero, there is no change taking place in the electron distribution, whereas in the regions where the function acquires a given numerical value, there would be changes in the distribution of added electrons. Thus, it becomes possible to associate the presence of a conduction band in the zones where the Fukui function acquires an average zero value.

Therefore, it is justified to assert that for the hexamer case, the conduction band of the polymer can be located within units 2 and 4 having electrons transferred with units 1 and 6, whereas for the trimer the active sites occur on the $N_{\underline{C}}$ in the central unit, with the conduction band present throughout the polymer. The results obtained by means of the potentiodynamic synthesis revealed the presence of a conducting polymer on the surface of the working electrode, as suggested by the charge increase that took place as a function of the number of cycles. Thus, this is assumed as the evidence of the growth of the conducting polymer and of the presence of a conducting band. The theoretical results of the function $f_{N_s}(r)$ for the hexamer corroborate the experimental behaviour observed, giving a clear indication that the suggested polymer structure is the most likely one for the 5Aphen. Furthermore, the structure is also consistent with the experimental results that evidence the growth of the polymer via direct incorporation of the monomers or oligomers.

IR spectroscopy may be a way to confirm with

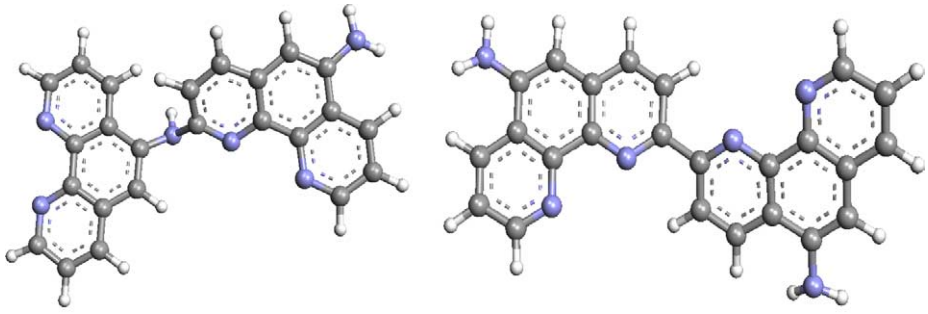

Fig. 13. Minimal energy conformation of two dimers of 5-amino-1,10-phenanthroline, obtained by AM1 calculations, corresponding to coupling modes of (a) $N_{\underline{C}}$–$C_{\underline{10}}$ and (b) $C_{\underline{1}}$–$C_{\underline{10}}$ atoms. The corresponding formation energy is also shown in each figure.

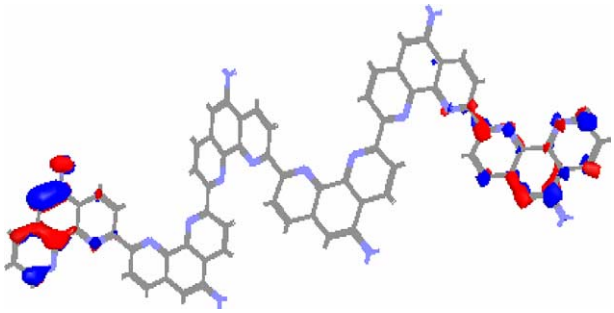

Fig. 15. Fukui function, $f_{N_s}(r)$, distribution of a 5Aphen hexamer. The nucleophilic site corresponding to the space region where f_{N_s} is positive, is indicated in blue and in red where it is negative, the electrophilic site.

experimental evidence that polymerisation occurs through couplings at the alpha carbons to nitrogen atoms in 5-amino-1,10-phenantroline. Therefore, in order to do this we first calculated the theoretical vibrational frequency spectrum (IR) by a single point semiempirical method (AM1) using the software Hyperchem 7.0 (Hypercube Inc., 1115 NW 4th Street, Gainesville, FL 32601, USA) of the dimer (previously fully optimized geometry). We found that the IR absorption frequency more closely related to the said bond fall within 1700–800 cm^{-1} wavenumber range. It is important to highlight that in this range the said bond has a preponderant participation however, others, mainly aromatic C=C bonds, also participate.

Then, we proceeded to obtain the experimental IR-spectrum of the polymer, potentiostatically deposited onto a vitreous carbon electrode, by using ATR (attenuated total reflectance) infrared spectroscopy using a Perkin–Elmer spectrophotometer, STIRGX system, coupled with a ATR diamond module, model Durasampl 1, with the aim to confirm this fact. The following, see Fig. 16, IR spectrum was obtained.

From this figure it is possible to note that the polymer exhibits an absorption peak at 1790 cm^{-1}, which, according to the previous discussion may indicate the existence of the analyzed bond. Moreover, Cunha et al. [37] have shown by high resolution STM that the self-assembled 1,10-phenantroline monolayer onto a single crystal electrode (Au(111)) is formed by polymer-like linear chains (see Fig. 4 in Ref. [37]), resembling the structure depicted in Fig. 15.

4. Conclusions

It has been shown that the electropolymerisation of the 5Aphen was carried out, potentiostatic and potentiodynamically onto glassy carbon, carbon paste, graphite-epoxy resin composite and polycrystalline gold electrodes. The formation of the polymeric film onto the surfaces of the glassy carbon and polycrystalline gold electrodes has been well described by the same electrochemical new phase formation mechanism that involves the simultaneous presence of adsorption and 3D diffusion-limited growth processes where the nucleation and growth process of the polymer, take place via direct incorporation of the monomers. From the theoretical study it was possible to describe a plausible oligomer structure that fulfilled with the experimental evidence found.

Acknowledgements

The authors wish to express their thanks to CONACYT for the funding given through projects: 46171-Q and 47178-F and to the Materials Department (UAM-A) through projects: 2260220 and 2260225. Also, JACM and RAB express their gratitude to CONACYT for the studentships given to pursue their postgraduate studies. This work was

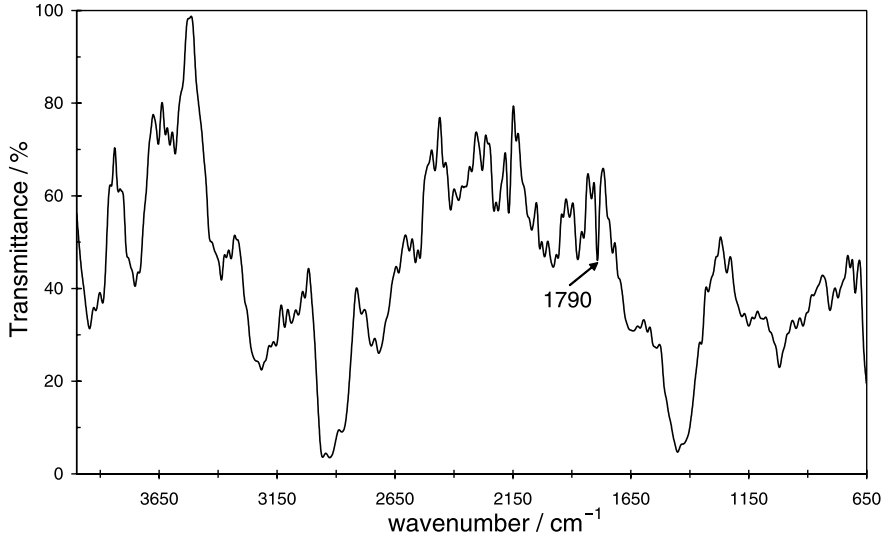

Fig. 16. IR spectrum of the polymeric film formed by electropolymerisation of the 5Aphen in the system: glassy carbon/2×10^{-3} M 5Aphen in sulphuric acid at pH = 0.3, after imposing a potential jump from the null current potential 177 mV to a 1500 mV during 200 s.

presented in partial fulfilment of JACM and RABs PhD degree's requirements. LG, ARH, MTRS, GRP, MRR and MPP, gratefully acknowledge the SNI for the distinction of their membership and the stipend received. The authors are indebted to Dr Jorge Mostany for his interest in this work and helpful discussions regarding the IR spectroscopy results.

References

[1] Álvarez Romero GA, Morales Pérez A, Rojas-Hernández A, Palomar-Pardavé M, Ramírez-Silva MT. Electroanalysis 2004;16(15): 1236–43.
[2] Galicia-Luis L, Rojas-Hernández A, Gómez-Hernández M, Ramírez-Silva MT. A novel pH sensor based on a conducting polymer formed from 5-amino-1,10-phenanthroline. In: Ramírez-Silva MT, Romero-Romo MA, Palomar-Pardavé ME, editors. Sensors and Chemometrics, Kerala, India: Research Signpost, 2001. pp. 65–73.
[3] Ramírez-Silva MT, Gómez-Hernández M, Pacheco-Hernández ML, Rojas-Hernández A, Galicia L. Spectrochimica Acta Part A 2004;60–64:781–9.
[4] Scharifker BR, Mostany J. J Electroanal Chem 1984;177:13–23.
[5] Scharifker BR, Mostany J, Palomar-Pardavé M, González I. J Electrochem Soc 1999;146(1005):1012.
[6] Philipp R, Retter U. Electrochim Acta 1995;40:1581–5.
[7] Li YG, Lasia A. J Electrochem Soc 1997;144:1979–88.
[8] Palomar-Pardavé M, González I, Batina N. J Phy Chem B 2000;104: 3545–55.
[9] Espinoza-Ramos LI, Hallen-López JM, Ramírez C, Arce E, Palomar-Pardavé M, Romero-Romo M. J Electrochem Soc 2002;149(12): B543–B50.
[10] Belamie E, Argoul F, Faure C. J Electrochem Soc 2001;148(4): C301–C9.
[11] Rajagopalan R, Iroh JO. Electrochim Acta 2001;46:2443–55.
[12] Schrebler R, Grez P, Cury P, Veas C, Merino M, Gómez H, et al. J Electroanal Chem 1997;430(1–2):77–90.
[13] Parr RG, Yang W. Density functional theory of atoms and molecules. New York: Oxford University Press; 1989.
[14] Gómez-Hernández M. Estudio de especiación química y electropolimerización del sistema 5-amino-1,10-fenantrolina en agua. Efecto de la concentración de H_3O^+ y Fe(II). Ms Sc Thesis UAM-Iztapalapa; 1999.
[15] Rojas-Hernández A, Ramírez-Silva MT, González I, Ibáñez J. J Chem Ed 1995;72:1099–105.
[16] Heinze J, Dietrich M. Cyclic voltammetry as a tool for characterizing conducting polymers. Mater Sci Forum 1989;42:63–78.
[17] Scharifker BR, Garcia-Pastoriza E, Marino W. J Electroanal Chem 1991;30:85–98.
[18] Mendoza-Huizar LH, Robles J, Palomar-Pardavé M. J Electroanal Chem 2003;545C:39–45.
[19] Garduño-Juárez RH, Romero-Romo M, Palomar-Pardavé M, Rojas-Hernández A, Ramírez-Silva MT. Mecanismo y cinética de formación electroquímica de un polímero conductor. Proceedings of the XV Congress of the "Sociedad Ibero-Americana de Electroquímica" Évora, Portugal: SIBAE, 2002. pp. 8–13.
[20] Garfias-García E, Romero-Romo M, Rojas Hernández A, Ramírez-Silva MT, Palomar-Pardavé M. Formación electroquímica de un polímero conductor base Pb-acetatos y caracterización mediante AFM. Proceedings of the XVIII Congress of the "Sociedad Mexicana de Electroquímica" Chihuahua Mexico: SMEQ, ISBN. 968-5742-01-4.
[21] Ramírez C, Arce EM, Romero-Romo M, Palomar-Pardavé M. Solid State Ionics 2004;169:81–5.
[22] Hölzle MH, Retter U, Kolb DM. J Electroanal Chem 1994;371:101.
[23] Scharifker BR, Fermín DJ. J Electroanal Chem 1994;365(1–2):35–9.
[24] Fermín DJ, Mostany J, Scharifker BR. Curr Top Electrochem 1993;2: 131–6.
[25] Nyasulu FWM, Mottola HA. J Electroanal Chem 1988;239:175.
[26] Mora MA, Galicia L, Mora-Ramirez MA. Int J Quantum Chem 2004; 97:98.
[27] De Gregori I, Bedioui F, Devynick J. J Electroanal Chem 1987;238: 197.
[28] Dewar MJS, Zoebisch EG, Healy EF, Stewart JP. J Am Chem Soc 1985;107:3902–9.
[29] Thompson MA, Zerner MC. J Am Chem Soc 1991;113:8210.
[30] Thompson MA, Glendening ED, Feller D. J Phys Chem 1994;98: 10465–76.
[31] Thompson MA, Schenter GK. J Phys Chem 1995;99:6374–86.
[32] Thompson MA. J Phys Chem 1996;100:14492–507.
[33] Fukui K. The world of quantum chemistry Daudel and Pullman ed USA. Proceedings of the first international congress of quantum chemistry held at menton 1974. p. 113–141.
[34] Galvan M, Vargas R. J Phys Chem 1992;96:1625.
[35] Galvan M, Vela A, Gazquez JL. J Phys Chem 1988;92:6470.
[36] Mendoza-Huizar LH, Palomar-Pardavé M, Robles J. J Mol Struct (Theochem) 2004;679:187–94.
[37] Cunha F, Jin Q, Tao NJ, Li CZ. Surf Sci 1997;389:19–28.